# Dye-Sensitized Photocells with Meso-Macroporous $TiO_2$ Film Electrodes

**Seigo Ito, Keiji Ishikawa,† Ching-Ju Wen,† Shoichiro Yoshida, and Tadashi Watanabe***

Institute of Industrial Science, The University of Tokyo, 7-22-1, Roppongi, Minato-ku, Tokyo 106-8558

†Department of Chemical System Engineering, Faculty of Engineering, The University of Tokyo, 7-3-1 Hongo, Bukyo-ku, Tokyo 113-8656

(Received March 13, 2000)

Meso-macroporous anatase $TiO_2$ films, described in a previous work, have been used for the first time as electrodes for dye-sensitized photoelectrochemical cells. The mesopores provide a large surface area that is favorable for efficient light absorption, and the macropores serve as pathways for diffusion of electroactive agents (EAAs). Although the introduction of macropores led to an improvement in the magnitude of the short-circuit photocurrent ($J_{sc}$), electron recombination on the $SnO_2$ substrate surface at the bottom of the macropores deteriorated the open-circuit voltage ($V_{oc}$). This unfavorable process has been depressed by applying a thin (200 to 300 nm) $TiO_2$ film between the meso-macroporous film and the $SnO_2$ substrate, to obtain finally a dye-sensitized photoelectrode with a $V_{oc}$ nearly identical with, and a $J_{sc}$ superior to, the values for a conventional porous $TiO_2$ film electrode.

Dye-sensitized solar cells using nanoparticles of $TiO_2$ for light-to-electricity conversion have been investigated extensively.[1—3] Figure 1a depicts the geometry and the charge transport process of such a cell, sensitized with a monolayer of Ru complex dye molecules adsorbed on the $TiO_2$ surface. The electrons injected into the $TiO_2$ conduction band migrate through the interconnecting network of $TiO_2$ particles, are collected by the conducting glass electrode, and then reduce $I_3^-$ to $I^-$ at the Pt counter electrode. The $I^-$ ion diffuses from the counter electrode into the porous $TiO_2$ film to reduce the oxidized dye molecule, thereby regenerating the original dye and completing the oxidation–reduction cycle.

A high light-to-electricity conversion efficiency at these porous electrodes results from a large surface area, 780 times that of a smooth electrode,[1] produced by the meso-sized (2 to 50 nm) pores[4] within the electrode. However, since the film thickness (ca. 10 μm) is $10^3$-fold greater than the diameter of the mesopores (ca. 10 nm), the walls of mesopores hinder the diffusion of electroactive agents (EAAs). Kebede and Lindquist[5] recently reported that the apparent diffusion coefficient of EAA in the mesopores is ten times smaller than that in the bulk solution. Although they estimated that the EAA diffusion is still rapid enough not to limit the dye-sensitized cell efficiency,[5—7] there are reports stating that the slow diffusion of EAA due to the high viscosity of the electrolyte lowers the cell output.[8,9] In view of this, several workers[10—14] have reported $TiO_2$ film electrodes possessing macro-sized pores, in an attempt to facilitate the EAA diffusion through the film layer. Such macroporous $TiO_2$ electrodes, however, inevitably have a smaller surface area that decreases the light absorption efficiency.[13,14]

In order to overcome this drawback, we have fabricated meso-macroporous anatase $TiO_2$ film electrodes from secondary submicroparticles,[15] prepared by a hydrothermal treatment yielding a stable $TiO_2$ colloid.[16] The mesopores provided a large surface area for dye adsorption, and the

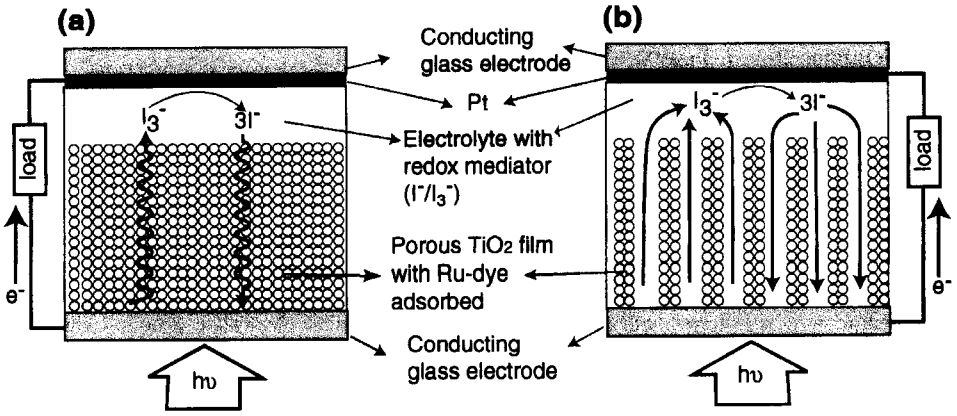


Fig. 1. Schematic illustrations of dye-sensitized solar cells with (a) mesoporous and (b) meso-macroporous $TiO_2$ films.

macropores were expected to facilitate the diffusion of EAA (Fig. 1b). The performance of these meso-macroporous electrodes in the dye-sensitized photocells was compared with those of a traditional mesoporous film,[1] a meso-macroporous film fabricated by iteration of coating and combusting, and a meso-macroporous film with a thin $TiO_2$ film underlayer on the $SnO_2$ substrate. The results demonstrate that the design of the pore structure of $TiO_2$ film electrodes leads to a substantial improvement in the dye-sensitized cell characteristics.

## Experimental

**Fabrication of Meso-Macroporous Film.** In research described in a companion paper,[15] a meso-macroporous $TiO_2$ electrode was prepared by applying four coatings of $TiO_2$ secondary submicroparticles[16] onto an $SnO_2$ coated glass and drying at 50 °C, followed by one-shot combustion at 270 °C for 2 h, and finally sintering at 450 to 550 °C in a tubular ceramic heater. This film is referred to as OC below. In the present work, OC was prepared by applying five coatings to further increase the specific surface area. Two different conditions (450 °C for 30 min: ($OC_{450°C}$) and 550 °C for 3 h: ($OC_{550°C}$)) were employed for heat treatment to examine the effects of crystallinity and surface area on the solar cell performance. Heating at 450 °C for 30 min yielded a large surface area (99.6 $m^2 g^{-1}$) with a small amount of brookite remaining; heating at 550 °C for 3 h yielded a smaller surface area (46.9 $m^2 g^{-1}$), a high degree of crystallization of anatase, and disappearance of the brookite phase.[15]

To compare and/or improve the dye-sensitized cell performance, three additional electrodes were prepared. One was a traditional mesoporous $TiO_2$ film electrode (called ME below),[1–3] prepared from a commercially available $TiO_2$ sol (Ti-Nanoxide T, Solaronix) and with a well-established preparation procedure.[6] The second (IC) was a meso-macroporous film electrode fabricated by five iterative coating-and-combustion sequences followed by calcination at 550 °C for 3 h, as shown in Fig. 2a. The third (OCT) was a meso-macroporous film electrode that carries a thin $TiO_2$ underlayer beneath an $OC_{550°C}$ film, prepared according to the scheme of Fig. 2b. Characterization of the OCT electrode will be detailed in Results and Discussion.

The morphologies of the films thus prepared were observed on a scanning electron micrograph (SEM, S-4500, Hitachi), where no metal-sputtering was needed because of the electron-reflecting effect of the electrically conductive $TiO_2$. The crystallinity of the porous $TiO_2$ electrodes was characterized by XRD (RINT 2100, Rigaku). The thickness of the thin $TiO_2$ underlayer was measured with a surface profiler (Dektak3, Solan). The surface area and pore size distribution of the $TiO_2$ films, degassed at 300 °C for 30 min in a vacuum, were measured by the nitrogen adsorption method (AUTOSORB-1, Quantachrome). The pore size distribution was modeled using the Barrett-Johner-Halenda (BJH) method on the desorption data.

**Dye-Sensitization Experiments.** A dye-sensitized cell was fabricated following the procedure described by Nazzerruddin et al.[2] A 0.2 M $TiCl_4$ aqueous solution was dropped onto a $TiO_2$ film electrode (0.25 $cm^2$), and the film was kept for 6 h in a closed casing (1 M = 1 mol $dm^{-3}$). The film was then washed with Milli-Q purified water, heated at 450 °C for 30 min to remove contaminants by combustion, and immersed in an ethanol solution of (*cis*-di(thiocyanato)-*N*,*N*′-bis(2,2′-bipyridyl-4,4′-dicarboxylic acid) ruthenium(II) (Solaronix) for 24 h. The amount of adsorbed dye was determined by a previously reported method.[2] After the dye adsorption, the film was soaked in *t*-butyl pyridine for 30 min. A 25-μm thick ionomer resin sheet (Surlyn1702, Du Pont) was used as a spacer of the sandwiched cell ($TiO_2$/spacer/Pt). A Pt counter electrode was sputtered onto a $SnO_2$ substrate with two small holes for injecting the electrolyte solution, a mixed solvent consisting of 0.3 M LiI+0.03 M $I_2$ in acetonitrile/3-methyl-2-oxazolidinone (90/10, v/v). After the electrolyte injection, the holes on the Pt electrode were plugged with a hot-melt film (Takemelt, Takeda Healthcare). The cells were then illuminated with an AM 1.5 (100 mW $cm^{-2}$) solar simulator (Yamada Electric), and the photocurrent–voltage characteristics were measured.

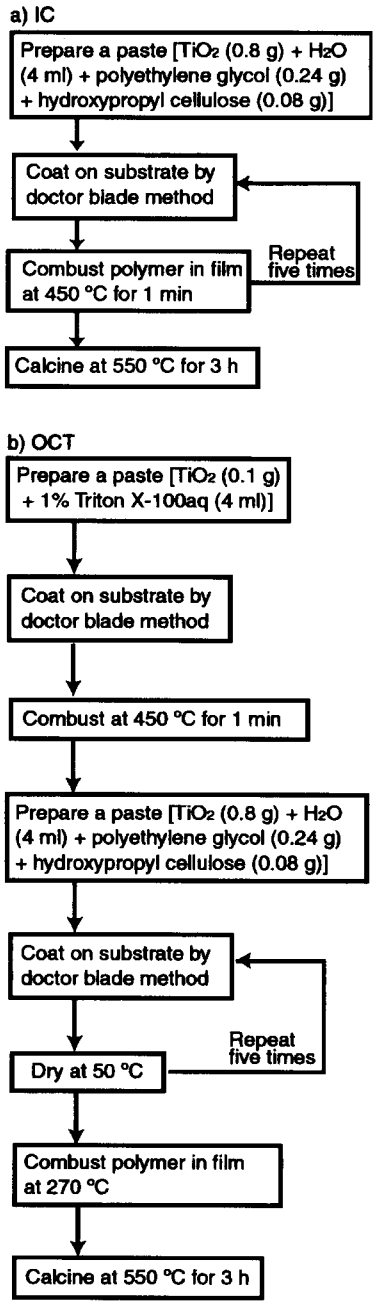


Fig. 2. Method for fabricating (a) an iteratively combusted meso-macroporous film (IC) and (b) a meso-macroporous film on a thin $TiO_2$ underlayer (OCT).

## Results

**Characterization of Porous $TiO_2$ Electrodes.** In an attempt to suppress the charge recombination on the $SnO_2$ substrate surface[17] while maintaining the macropores for the EAA diffusion within the meso-macroporous $TiO_2$ film, we covered the $SnO_2$ surface with a thin (200 to 300 nm) $TiO_2$ film before depositing an $OC_{550°C}$ film, to obtain an OCT electrode. Figure 3 depicts the SEM photographs for a bare $SnO_2$ surface (a), the surface of the thin $TiO_2$ layer (b), and that of the meso-macroporous film (c). As is seen, the thin $TiO_2$ layer is composed of fine particles of about 10 nm in diameter, and is similar to a conventional mesoporous film.[1,2] Furthermore, the film neatly covered the underlying $SnO_2$ surface, and was expected to effectively hinder charge recombination that tends to deteriorate the open-circuit voltage $V_{oc}$.

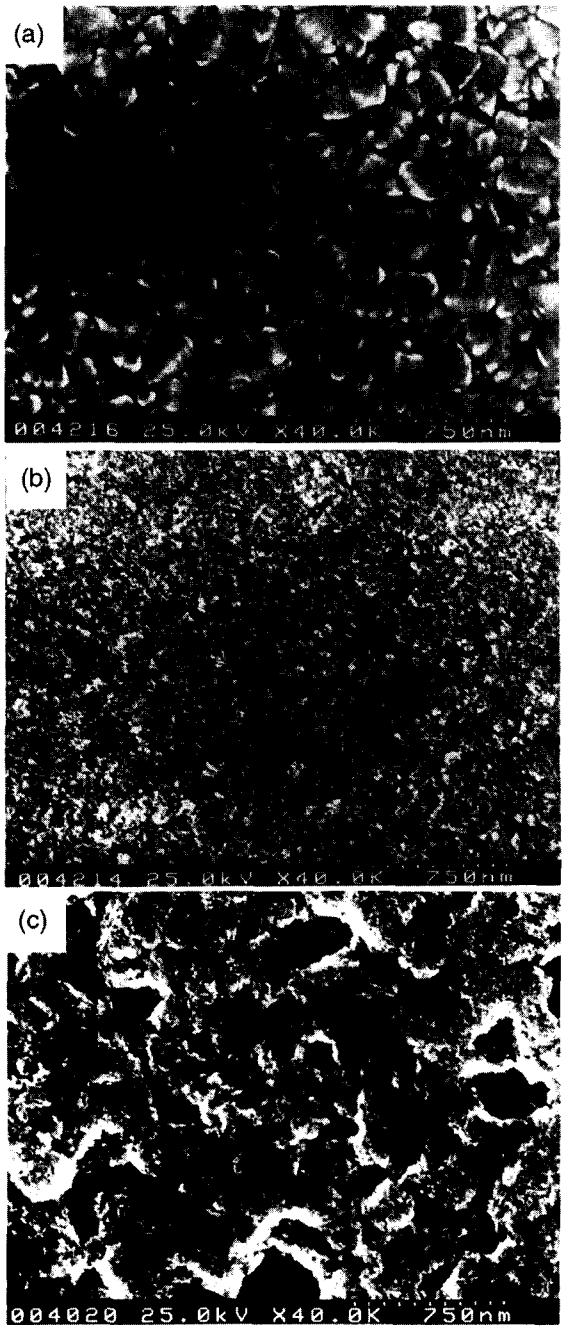


Fig. 3. Scanning electron micrographs of (a) a bare $SnO_2$ substrate, (b) a thin $TiO_2$ film, and (c) a meso-macroporous film.

Figure 4 shows the pore size distribution of the $TiO_2$ films. The surface area, the roughness factor, and the amount of adsorbed dyes among five electrodes are summarized in Table 1. The correlation between the roughness factor and the dye adsorption is fair. The slight difference might be due to the presence of very small pores to which the dye molecules cannot adsorb. The pore size of the ME electrode is ca. 10 nm, being below 20 nm, while the pore size of other $TiO_2$ electrodes are larger than that of ME, ranging widely from 5 nm to 100 nm. As the roughness factor of the ME electrode is consistent with the reported data,[1] the ME electrode is employed as a standard $TiO_2$ electrode for comparison. However, we confirmed that the roughness factor and the dye adsorption of the ME electrode are much less than those of other electrodes. For the OC electrodes, the pore size distribution increased, probably due to densification and necking, when the calcination temperature was raised from 450 °C to 550 °C.[15,18] There is no appreciable difference in the pore size and dye adsorption between the $OC_{550°C}$ and OCT electrodes, though the roughness factors differ to some extent (Fig. 4, Table 1). In the IC electrode, pores exceeding 20 nm seemed to be plugged by iteration of coating and combustion. Although there were distinct differences between the pore size distribution of the $OC_{550°C}$ and IC electrodes, the roughness factor and the dye adsorption were found comparable.

The crystallinities of IC and OCT were the same as that of $OC_{550°C}$ (anatase).[15] It has already been proven that the crystallinity of $OC_{450°C}$ is lower than that of $OC_{550°C}$.[15] In the present investigation, it became apparent that the half-value

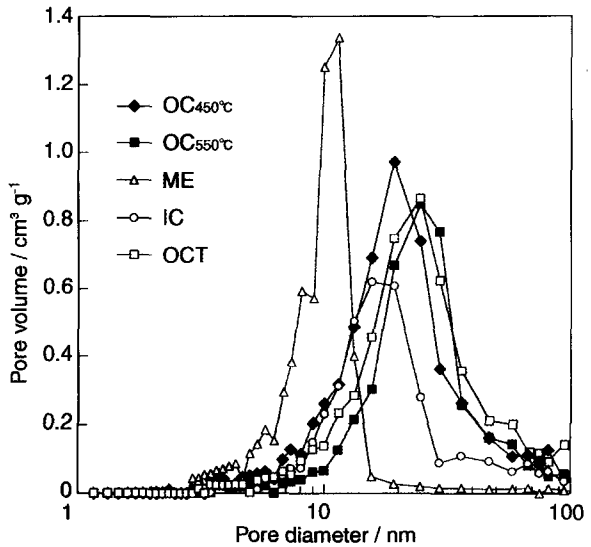


Fig. 4. Pore size distribution (differential volume) of $OC_{450°C}$, $OC_{550°C}$, ME, IC, and OCT.

Table 1. Physical Parameters and Photovoltaic Data for Five Porous $TiO_2$ Electrodes

| Film | $OC_{450°C}$ | $OC_{550°C}$ | ME | IC | OCT |
|---|---|---|---|---|---|
| Temperature/°C | 450 | 550 | 450 | 550 | 550 |
| Time/h | 0.5 | 3 | 0.5 | 3 | 3 |
| Surface area/$m^2\ g^{-1}$ | 84.4 | 52.2 | 105 | 57.2 | 70.5 |
| Roughness factor | 2300 | 1400 | 723 | 1600 | 1900 |
| Amount of adsorbed Dyes/$10^{-7}$ mol $cm^{-2}$ | 2.5±0.2 | 2.1±0.2 | 0.68±0.02 | 1.9±0.1 | 2.0±0.1 |
| $V_{OC}$/mV | 550±30 | 554±6 | 611±1 | 568±5 | 606±10 |
| $J_{SC}$/mA | 8.9±1.2 | 10.0±0.1 | 9.2±0.8 | 7.7±0.2 | 11.1±0.4 |
| $\eta$/% | 2.9±0.2 | 3.1±0.2 | 3.4±0.1 | 2.7±0.2 | 3.8±0.1 |

width of the XRD pattern of the ME electrode is greater than that of the $OC_{450°C}$ electrode, suggesting that $OC_{450°C}$ should consist of larger crystallized particles or higher crystallinity than ME.

**Photovoltaic Characteristics of Each $TiO_2$ Film** Figure 5 shows the photovoltaic characteristics of dye-sensitized cells with OC film electrodes prepared by heating at 450 °C for 30 min ($OC_{450°C}$) and at 550 °C for 3 h ($OC_{550°C}$). For the former, with a roughness factor of 2300, the short-circuit photocurrent ($J_{sc}$) was 8.9±1.2 mA $cm^{-2}$; the open-circuit photovoltage ($V_{oc}$) was 550±30 mV; and the light-to-electricity conversion efficiency ($\eta$) was 2.9±0.2% (Table 1). In contrast, for the latter electrode with a reduced roughness factor of 1400, $J_{sc}$ was 10.0±0.1 mA $cm^{-2}$, $V_{oc}$ was 554±6 mV, and $\eta$ was 3.1±0.2% (Table 1). As described elsewhere,[15] the degree of heat treatment affected the crystallinity of the resulting $TiO_2$ film; a tiny but non-negligible brookite peak was discernible in the XRD pattern for the film prepared by heating at 450 °C for 30 min, while the film heat-treated at 550 °C for 3 h was practically brookite-free.

In view of this, the improved cell performance despite a smaller specific surface area and with an electrode prepared at a higher heat-treatment temperature is most probably related to the progress of anatase phase purification, where the electron trapping efficiency and the energy barrier are both reduced because of the disappearance of the brookite phase. A similar observation has been reported by Park et al.,[19] who demonstrated that a mesoporous rutile electrode prepared by annealing at 500 °C for 30 min gave a cell performance better than that by annealing at 300 °C for 30 min. Based on this finding, the meso-macroporous $TiO_2$ film electrodes described hereafter were fabricated by heating at 550 °C for 3 h.

Figure 6 illustrates the dye-sensitization characteristics of cells constructed with $OC_{550°C}$, ME, IC and OCT electrodes, where the curve for $OC_{550°C}$ is the same as that in Fig. 5. The output parameters $J_{sc}$, $V_{oc}$, and $\eta$ were 9.2±0.8 mA $cm^{-2}$, 611±1 mV, and 3.4±0.1% for ME, 7.7±0.2 mA $cm^{-2}$, 568±0.5 mV, and 2.7±0.2% for IC and 11.1±0.4 mA $cm^{-2}$, 606±10 mV, and 3.8±0.1% for OCT electrodes (Table 1). Compared with the conventional ME-based cell, the value of $J_{sc}$ is larger for $OC_{550°C}$ and smaller for IC. Note that $J_{sc}$ and $\eta$ of OCT are superior to those attained with the ME electrode (curve d) fabricated both with the materials and

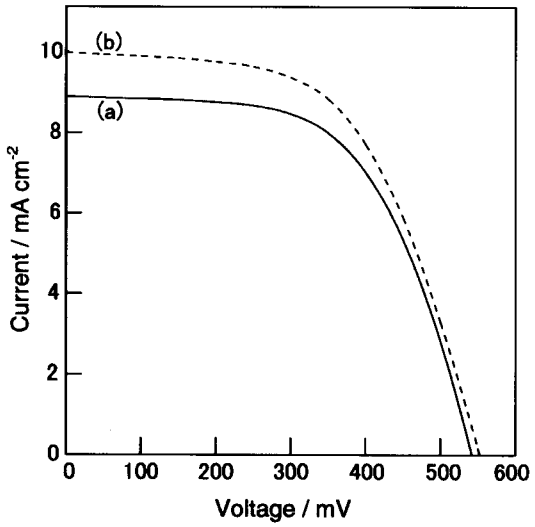


Fig. 5. Photocurrent-voltage characteristics of solar cells with a meso-macroporous anatase film prepared by sintering (a) at 450 °C for 30 min ($OC_{450°C}$) and (b) at 550 °C for 3 h ($OC_{550°C}$), irradiated with an AM 1.5 solar simulator.

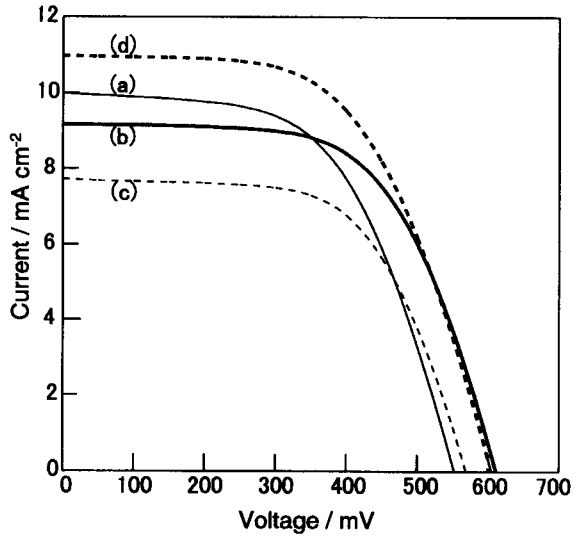


Fig. 6. Photocurrent-voltage characteristics of solar cells with (a) a meso-macroporous film fabricated by one-shot combustion ($OC_{550°C}$), (b) a mesoporous film (ME), (c) an iteratively combusted meso-macroporous film (IC), and (d) $OC_{550°C}$ with a thin $TiO_2$ underlayer (OCT) irradiated with an AM 1.5 solar simulator.

procedures recommended by the Grätzel group.[1,2,6]

## Discussion

**Comparison of $OC_{550°C}$ and ME Electrodes.** Compared to a conventional ME-based cell, the value of $J_{sc}$ is larger for $OC_{550°C}$ (Fig. 6, Table 1). The results can be explained as follows. First, the macropore sizes facilitate EAA diffusion through the $TiO_2$ layer (Fig. 1b). Second, the dye adsorption on the $OC_{550°C}$ electrode is about three times as large as that on the ME electrode (Table 1). Third, the high crystallinity of $OC_{550°C}$ should contribute to effective electron mobility, affecting the dye-sensitization (Fig. 5).[19] However, the effect of crystallinity on electron mobility is still controversial.

In contrast, the value of $V_{OC}$ for $OC_{550°C}$ is smaller than that of ME. The magnitude of the open-circuit photovoltage $V_{oc}$ is controlled by charge recombination at the electrode-redox electrolyte interface.[6] Electrons are injected from excited dye molecules to the $TiO_2$ conduction band and are then collected by the underlying $SnO_2$ electrode, while the oxidized dye molecules $D^+$ are reduced by $I^-$ in the electrolyte. When the $I^-$ concentration is high enough, the recombination between $D^+$ and the $TiO_2$ conduction electrons is usually negligible.[20,21] Hence, the most important charge recombination, leading to a decreased photovoltage, has been assessed to be the reduction of $I_3^-$ to $I^-$:[22]

$$2e^- + I_3^- \rightarrow 3I^- \quad (1)$$

The electrons in Eq. 1 are supplied directly from the $TiO_2$ conduction band and/or from the $SnO_2$ conduction band after electron cascading from $TiO_2$.[17] The value of $V_{oc}$ for the $OC_{550°C}$ electrode is smaller than that for the ME electrode (Fig. 6). Since the $OC_{550°C}$ electrode was prepared by one-shot combustion of the polymers, the macropore may well extend from the film surface down to the $SnO_2$ substrate surface, which hence is in direct contact with the electrolyte when assembled into a cell. Therefore the charge recombination (Eq. 1) is facilitated, and this in turn lowers the magnitude of $V_{oc}$ (Fig. 7a). However, since the pores of the ME electrode on the $SnO_2$ substrate are small, it may be difficult to generate the charge recombination (Fig. 7b).

**Photovoltaic Characteristic of IC.** Since the differences of the photovoltaic characteristics between $OC_{550°C}$ and ME as such are not evidence of effective EAA diffusion in the macropores, the apparent diffusion coefficients of EAA in these porous materials should be detected. Kebede and Lindquist[5] reported that the apparent diffusion coefficient in a $TiO_2$ filter membrane without a support substrate was due to the porosity of the $TiO_2$ films. However, since this film on the $SnO_2$ substrate had some cracks,[15] the surface area of the unhusked $SnO_2$ cannot be estimated from the pore size.

Thus, instead of electrochemical measurement of the apparent diffusion coefficient, we discussed the photovoltaic characteristics of IC. The iterative coating and combusting sequences should cause plugging in the macropores (Fig. 7c). Such plugging was supported by the decreased pore size distribution (Fig. 4). $J_{SC}$ of the IC electrode decreased by 20%, which was much more than expected from dye adsorption (10% decrease) when compared with that of $OC_{550°C}$. Hence, the smaller $J_{sc}$ for the IC electrode (Fig. 6, Table 1) may be a result of EAA diffusion hindrance by such plugging.

The $V_{oc}$ value for the IC electrode is between those for ME and $OC_{550°C}$ electrodes. This may reflect the occurrence of partial blocking (Fig. 7c) of the back electron transfer (Eq. 1) due to the plugging of the macropores.

**Photovoltaic Characteristics of Novel Designed Electrode: OCT.** In order to prevent the back electron transfer at the $SnO_2$ surface, the surface of the $SnO_2$ substrate unhusked in the macropore is coated with a thin $TiO_2$ underlayer. The thin $TiO_2$ underlayer should help control the charge recombination (Fig. 7d). Figure 6d shows the photovoltaic characteristics of the OCT electrode. As expected, the value of $V_{OC}$ for OCT increased drastically, giving the same value as for ME. Therefore, the deposition of the thin $TiO_2$ underlayer seems to efficiently prevent the charge recombination between EAA and the $SnO_2$ substrate.

Although a smaller amount of dye molecules was adsorbed on the OCT electrode than on the $OC_{550°C}$ electrode, the $J_{SC}$ of OCT is larger than that of $OC_{550°C}$ by ca. 10% (Table 1). However, preventing charge recombination does not improve $J_{CS}$.[6] Therefore, the improvement of the photocurrent seems to be due to the enhancement of the electron collecting efficiency. As the crystallinity of these $TiO_2$ electrodes is identical, the difference of $J_{SC}$ should be due to the thin $TiO_2$ underlayer. This may be explained as follows. First, the effective formation of a charge depletion layer at the $TiO_2/SnO_2$ interface with the thin $TiO_2$ underlayer may contribute to effective charge separation at the OCT electrode.[23,24] Second,

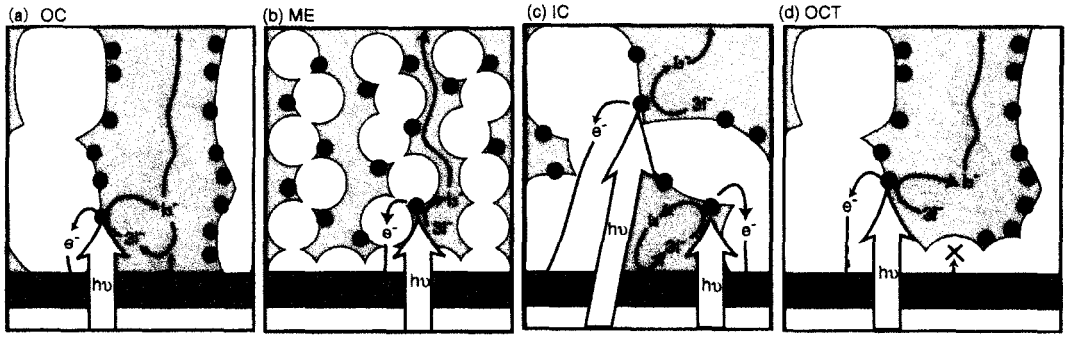


Fig. 7. Electron and mass transfers at the $TiO_2$/substrate interfacial regions for the four electrodes (see text).

the $TiO_2$ underlayer may also prevent the direct interaction of ionic species with the $SnO_2$ substarte.[24]

Grätzel et al.[1,2] reported the conversion efficiency ($\eta$) to be ca. 10% for dye-sensitized cells constructed with an ME electrode. Later works by other researchers questioned the reproducibility of $\eta = 10\%$; for example, a value of $\eta = 4.8\%$ has been obtained by Miyazaki et al.[25,26] In the present work, the value of $\eta$ was 3.4% for an ME electrode under supposedly the same experimental conditions. However, since the photovoltaic parameters undergo changes by subtle and occasionally uncontrollable drifts of intensity and the spectrum of the light source employed, we presume that the apparent difference between $\eta = 3.4\%$ and $\eta = 4.8\%$ is of little significance. We would like to emphasize again that, in going from the ME to the OCT electrode, $J_{sc}$ has been improved by a factor of 1.2, to yield an $\eta = 3.8\%$. This demonstrates that the pore structural design of $TiO_2$ electrodes is a key element in constructing efficient dye-sensitized solar cells, and will find applications in future work on related subjects.

The authors are indebted to Mr. K. Kita, Department of Chemical System Engineering, The University of Tokyo, for the photovoltaic measurements with the solar simulator, and to Prof. S. Yanagida, Material and Life Science Graduate School of Engineering, Osaka University, for the surface area and pore distribution measurements.

## References

1 B. O'Regan and M. Grätzel, *Nature (London)*, **353**, 737 (1991).

2 M. K. Nazzerruddin, A. Kay, I. Podicio, R. Humphy-Baker, E. Müller, P. Liska, N. Vlachopoulos, and M. Grätzel, *J. Am. Chem. Soc.*, **115**, 6382 (1993).

3 U. Bach, D. Lupo, P. Comte, J. E. Moser, F. Weissörtel, J. Salbeck, H. Spreitzer, and M. Grätzel, *Nature (London)*, **395**, 583 (1998).

4 C. A. C. Sequeira and M. J. Hudson, "Multifunctional Mesoporous Inorganic Solids, Mathematical and Physical Sciences," Vol. 400 Kluwer: Dordrecht, The Netherlands (1993), Vol. 400, p. 4.

5 Z. Kebede and S.-E. Lindquist, *Sol. Eng. Mater. Sol. Cells*, **51**, 291 (1998).

6 S. Y. Huang, G. Schlichthörl, A. J. Nozik, M. Grätzel, and A. J. Frank, *J. Phys. Chem. B*, **101**, 2576 (1997).

7 N. Papageorgioiu, C. Barbé, and M. Grätzel, *J. Phys. Chem. B*, **102**, 4156 (1998).

8 N. Papageorgioiu, Y. Athanassov, M. Armand, P. Bonhôte, H. Pettersson, A. Azam, and M. Grätzel, *J. Electrochem. Soc.*, **143**, 3099 (1996).

9 O. Kohle, M. Grätzel, A. F. Meyer, and T. B. Meyer, *Adv. Mater.*, **9**, 904 (1997).

10 J. E. G. J. Wijnhoven and W. L. Vos, *Science*, **281**, 802 (1998).

11 B. T. Holland, C. F. Blanford, and A. Stein, *Science*, **281**, 538 (1998).

12 O. D. Velev, T. A. Jede, R. F. Lobo, and A. M. Lenhoff, *Nature (London)*, **389**, 448 (1997).

13 R. A. Caruso, M. Giersig, F. Willig, and M. Antonietti, *Langmuir*, **14**, 6333, (1998).

14 R. A. Caruso, M. Giersig, F. Willig, and M. Antonietti, *Ber. Bunsenges. Phys. Chem.*, **102**, 1540, (1998).

15 S. Ito, S. Yoshida, and T. Watanabe, *Bull. Chem. Soc. Jpn.*, **73**, 1933 (2000).

16 S. Ito, S. Yoshida, and T. Watanabe, *Chem. Lett.*, **2000**, 70.

17 C. Naser, P. V. Kamat, and S. Hotchandani, *J. Phys. Chem. B*, **102**, 10047 (1998).

18 C. J. Barbé, F. Arendse, P. Comte, M. Jirousek, F. Lenzmann, V. Shklover, and M. Gärtzel, *J. Am. Ceram. Soc.*, **80**, 3157 (1997).

19 N. G. Park, G. Schlichthorl, J. Van-de-Lagemaat, H. M. Cheong, A. Mascarenhas, and A. J. Frank, *J. Phys. Chem. B*, **103**, 3308 (1999).

20 A. Hagfeldt, S.-E. Lindquist, and M. Gärtzel, *Sol. Eng. Mater. Sol. Cells*, **32**, 245 (1994).

21 A. Hagfeldt and M. Gärtzel, *Chem. Rev.*, **95**, 49 (1995).

22 M. Gärtzel and K. Kalyanasundaram, *Curr. Sci.*, **66**, 706 (1994).

23 K. Schwarzbug, F. Willing, *J. Phys. Chem. B*, **103**, 5743 (1999).

24 F. Pichot and B. A. Gregg, *J. Phys. Chem. B*, **104**, 6 (2000).

25 Y. Miyazaki, Meeting of Material Department of Japan Ceramics Society (1996).

26 Y. Miyazaki, Z. Kamiya, M. Matsumoto, K. Matsuhiro, Y. Takaoka, S. Murasawa, 4th Workshop of High Effective Solar Cells, Nara, Japan (1994).